

THE DISCOVERY OF THE MOST METAL-RICH WHITE DWARF: COMPOSITION OF A TIDALLY DISRUPTED EXTRASOLAR DWARF PLANET

P. DUFOUR¹, M. KILIC², G. FONTAINE¹, P. BERGERON¹, F.-R. LACHAPELLE¹, S. J. KLEINMAN³, S. K. LEGGETT³

Draft version August 16, 2018

ABSTRACT

Cool white dwarf stars are usually found to have an outer atmosphere that is practically pure in hydrogen or helium. However, a small fraction have traces of heavy elements that must originate from the accretion of extrinsic material, most probably circumstellar matter. Upon examining thousands of Sloan Digital Sky Survey spectra, we discovered that the helium-atmosphere white dwarf SDSS J073842.56+183509.6 shows the most severe metal pollution ever seen in the outermost layers of such stars. We present here a quantitative analysis of this exciting star by combining high S/N follow-up spectroscopic and photometric observations with model atmospheres and evolutionary models. We determine the global structural properties of our target star, as well as the abundances of the most significant pollutants in its atmosphere, i.e., H, O, Na, Mg, Si, Ca, and Fe. The relative abundances of these elements imply that the source of the accreted material has a composition similar to that of Bulk Earth. We also report the signature of a circumstellar disk revealed through a large infrared excess in *JHK* photometry. Combined with our inferred estimate of the mass of the accreted material, this strongly suggests that we are witnessing the remains of a tidally disrupted extrasolar body that was as large as Ceres.

Subject headings: stars: abundances – stars: atmospheres – stars: evolution – white dwarfs

1. INTRODUCTION

The vast majority of stars, some 97% of them, start their lives with masses less than about $8 M_{\odot}$. After going through mass loss episodes in the red giant phases, these stars ultimately run out of thermonuclear fuel and end up as compact objects known as white dwarfs. The white dwarf stars are characterized by masses around $0.6 M_{\odot}$ and dimensions comparable to that of the Earth, and they slowly cool off over periods of billions of years by radiating away the remaining thermal energy left in their core. Most of them are composed mainly — more than 99% of their mass — of carbon and oxygen, the products of hydrogen and helium nuclear burning. However, the processes of nuclear fusion and mass loss do not destroy or evaporate 100% of the hydrogen and helium that were initially present in the star at birth. Since the surface gravity of a white dwarf is extremely high ($\log g \sim 8$), light elements such as hydrogen and helium float to the surface in enough quantities to form an optically thick photosphere, while heavier elements sink rapidly out of sight. It is this efficient gravitational separation mechanism that is responsible for the high purity of the hydrogen or helium found in the atmospheres of most white dwarfs.

Traces of heavy elements are sometimes detected spectroscopically in the atmospheres of cool white dwarfs where radiative levitation or residual stellar winds no longer operate. Since their gravitational settling timescales are much shorter than the evolutionary cooling time, these elements cannot be primordial and

must have accreted relatively recently (metals sink on timescales of at most a few million years, while white dwarfs cool for several billion years, Paquette et al. 1986).

Passage through clouds in the interstellar medium (ISM) was, until recently, the commonly accepted scenario to explain the atmospheric pollution of these white dwarfs. However, two weaknesses in this hypothesis have been 1) the amount of hydrogen accreted onto helium-atmosphere stars is found to be several orders of magnitude lower than that of metals (Wolff et al. 2002; Dufour et al. 2007) despite the fact that the ISM is mostly constituted of hydrogen, and 2) investigations of the galactic positions and kinematics of white dwarfs with traces of metals all failed to show any evidence of an interaction with the ISM (Aannestad et al. 1993; Kilic & Redfield 2007; Farihi et al. 2010).

The last decade has seen the rise of a new paradigm as observations at infrared wavelengths revealed the presence of dusty disks orbiting the most metal-rich white dwarfs (Becklin et al. 2005; Kilic et al. 2005, 2006; von Hippel et al. 2007; Jura et al. 2007a,b; Farihi et al. 2009). It now appears, in all likelihood, that the heavy elements in most, if not all, polluted cool white dwarfs are accreted from this orbiting reservoir whose origin is explained by the tidal disruption of one or many orbitally perturbed asteroids (Debes & Sigurdsson 2002; Jura 2003, 2006, 2008). This alternative model also naturally explains the lack of correlation with the ISM and the small amount of hydrogen in the accreting material.

Traces of metals in the atmospheres of cool helium-rich white dwarfs are usually revealed only by the presence of the broad Ca II H and K absorption lines in the optical (see Dufour et al. 2007, and references therein), and very few stars show other heavy elements (note that observations in the ultraviolet part of the electromagnetic spec-

dufourpa@astro.umontreal.ca

¹ Département de Physique, Université de Montréal, Montréal, QC H3C 3J7, Canada

² Smithsonian Astrophysical Observatory, 60 Garden St., Cambridge, MA 02138, USA

³ Gemini Observatory, Northern Operations Center, Hilo, HI 96720, USA

trum, unfortunately available only for a few objects, see Wolff et al. 2002; Friedrich et al. 1999; Koester & Wolff 2000, reveal traces of a few more elements, with the strongest transitions being due to C, Mg, Si and Fe).

In a few rare cases, however, lines from a handful of elements can be observed in the optical. GD 362 and GD 40 (see Figure 1) are two of the most heavily polluted helium-rich white dwarfs currently known. Both of these stars also possess infrared emitting debris disks (Kilic et al. 2005; Jura et al. 2007a,b) which are believed to be the remains of a single tidally disrupted minor body (Jura 2006, 2008). Pioneering analyses of these two stars, based on Keck high resolution observations, have led to the determination of the relative abundances of 16 and 9 elements respectively (Zuckerman et al. 2007; Klein et al. 2010). The abundance patterns for these two objects are remarkably consistent with the idea that the source of the material is asteroids with a composition similar to that of Bulk Earth (Zuckerman et al. 2007; Klein et al. 2010). Studies of heavily polluted white dwarfs can thus offer a unique opportunity to learn about the chemistry of rocky extrasolar planet, asteroid belts, and their subsequent dynamical evolution following the red giant phases. As such, it is of utmost importance to increase the sample of white dwarfs with a comprehensive set of measured element abundances.

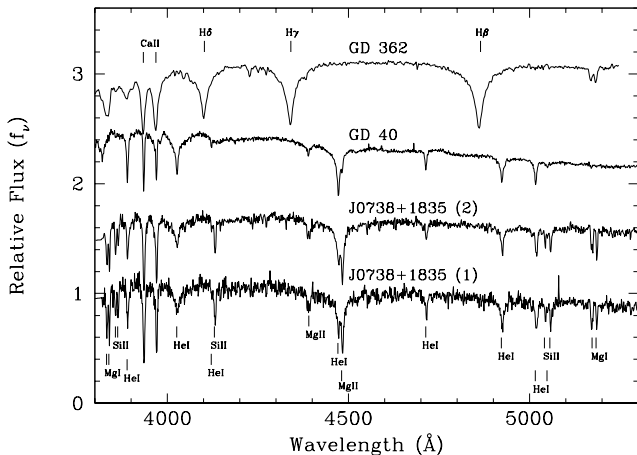


FIG. 1.— Medium resolution spectra of J0738+1835, GD 40, and GD 362. The two spectra of J0738+1835 and that of GD 40 are from SDSS, while the spectrum of GD 362 is taken from Gianninas et al. (2004).

In what follows, we present a detailed analysis of SDSS J073842.56+183509.6 (hereafter J0738+1835), the most metal-rich white dwarf discovered so far. In § 2, we describe the observations. Our detailed analysis follows in § 3, and the results are discussed and summarized in § 4.

2. TARGET SELECTION AND OBSERVATIONS

Recently, thanks to the Sloan Digital Sky Survey (SDSS), the number of spectroscopically identified white dwarfs has increased spectacularly (more than tenfold, and still counting, Kleinman et al. 2010, in preparation, see also Eisenstein et al. 2006), thus providing a large sample of potential candidates amenable to de-

tailed chemical analysis. In order to find such candidates, we selected from the SDSS 7th data release all spectroscopic objects with $g < 19.5$ mag that fall within the color space for white dwarf stars. These spectra were then visually inspected and classified into the various known white dwarf spectral types. It is while completing this exercise that the remarkable spectrum of SDSS J073842.56+183509.6 came to our attention (see Figure 1). J0738+1835 is a DBZ white dwarf that shows not only the usual Ca II H and K lines, but also several exceptionally strong lines of O, Fe, Mg and Si. Remarkably, note that the Mg II $\lambda 4481$ line is deeper than He I $\lambda 4471$, a unique feature among known polluted white dwarfs. The severity of the metallic pollution of J0738+1835 is particularly striking when its spectrum is compared to those of GD 362 and GD 40, two objects already known to be among the most polluted helium-rich white dwarfs currently identified (see Figure 1). Hence, J0738+1835 is a white dwarf star that offers great potential for a precise measurement of circumstellar material composition, and it is only the third helium-rich white dwarf (after GD 362 and GD 40) for which such a detailed analysis is possible from optical spectroscopy.

The SDSS photometric magnitudes, in the *ugriz* system, are $u = 17.527 \pm 0.014$, $g = 17.577 \pm 0.009$, $r = 17.822 \pm 0.009$, $i = 18.077 \pm 0.010$ and $z = 18.321 \pm 0.025$, suggesting an effective temperature in the 13,000–15,000 K range, depending on the amount of reddening that is assumed. Two spectra of this object, covering the 3800–9200 Å region at a resolution of ~ 3 Å FWHM are available from the SDSS archive. The SDSS-Modified Julian Date, plate and fiber ID number for these two spectra are respectively 53431-2054-346 and 54495-2890-354. These two original SDSS spectra of J0738+1835 presented in Figure 1 are too noisy for a precise determination of the atmospheric parameters (effective temperature, surface gravity, and abundances of the various elements). We thus, as a first step, secured a new medium resolution high S/N spectrum on UT 2009, November 19, using the 6.5 m MMT telescope on Mount Hopkins, Arizona, equipped with the Blue Channel Spectrograph. We used a 1" slit and the 500 line mm^{-1} grating in first order to obtain spectra with a wavelength coverage of 3500 – 6630 Å and a dispersion of 1.2 Å per pixel. All spectra were obtained at the parallactic angle. We used He-Ne-Ar comparison lamp exposures and blue spectrophotometric standards (Massey et al. 1988) for wavelength and flux calibration, respectively.

In order to verify if an emitting debris disk is present (see below), infrared observations are needed. We obtained *JHK* photometry of J0738+1835 using the Near Infra-Red Imager and Spectrometer (NIRI) on Gemini-North. These observations were performed on 2010, January 03 as part of the Director’s discretionary time program GN-2009B-DD-8. We used a 13 position dither pattern with 21–30 s exposures. We do not detect any sources above the background within 10" of the target. We used the Gemini/NIRI package in IRAF to reduce the data and the UKIRT faint standards (Leggett et al. 2006) to calibrate the photometry. The derived magnitudes, in the Mauna Kea photometric system, are $J = 17.965 \pm 0.031$, $H = 17.758 \pm 0.033$ and $K = 17.327 \pm 0.034$ (or 0.1034 ± 0.0031 mJy, 0.0791 ± 0.0026 mJy and

0.0752 ± 0.0025 mJy respectively).

3. DETAILED ANALYSIS

3.1. Model Atmospheres and Fitting Technique

The standard technique to determine the atmospheric parameters for helium-rich white dwarfs is to perform a χ^2 minimization of the normalized He I line profiles using a grid of synthetic spectra. However, in the case of J0738+1835, most of the He I lines are contaminated by heavy element absorption and finding good normalization points in the continuum is difficult due to the presence of numerous metallic lines. Moreover, metallic absorptions have a significant impact on the thermodynamic structure of the models, making estimations of the effective temperature and gravity from the He I lines alone unreliable. For example, in Figure 2, we show the influence of metals on the temperature and pressure structure of a $\log g = 8$, $T_{\text{eff}} = 14,000$ K model atmosphere. This effect is explained mostly by the flux redistribution due to line blanketing in the UV. We find that the iron lines provide the dominant contribution in that regard: for example, the thermodynamic structure of a model calculated without the iron line opacity is much closer to that of a pure helium model.

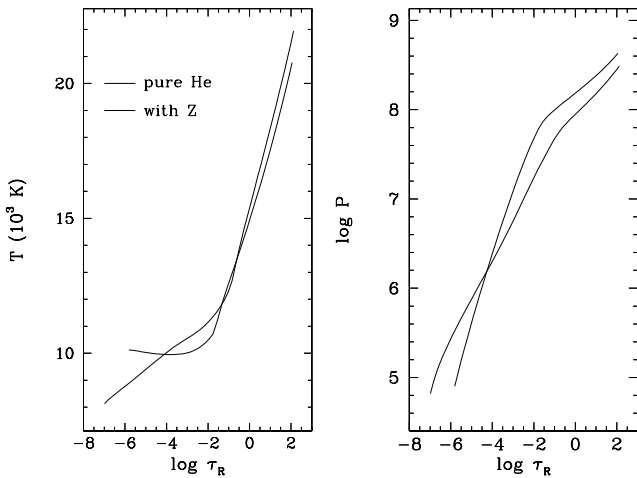


FIG. 2.— Temperature and pressure as a function of the Rosseland optical depth for white dwarf model atmosphere with $T_{\text{eff}} = 14,000$ K and $\log g = 8.0$. Thick line is for a pure helium atmosphere while the thin line is for a helium-rich atmosphere that includes traces of heavy elements ($\log(\text{Ca}/\text{He}) = -7.0$ with the abundances of other elements relative to Ca set as described in the text).

In this connection, it is interesting to note that our own fit of an optical SDSS spectrum of GD 40 (another DBZ star analysed in depth by Klein et al. 2010), using only the He I lines as in the standard approach and assuming $\log g = 8.0$ and a pure helium atmosphere, gives $T_{\text{eff}} = 15,180$ K, very similar to the 15,300 K of Voss et al. (2007). In contrast, a fit with a grid that includes heavy elements yields an effective temperature up to 1000 K cooler, depending on the exact amount of metals assumed. This should serve as a warning concerning the use of pure helium atmospheres for the analysis of such stars.

Given those circumstances, we prefer to fit simultaneously the He I lines and the numerous iron lines. This

is performed by fitting the whole spectrum with the solid angle, effective temperature, surface gravity, and the abundance of iron as free parameters. In order to take into account, to first order, the effect of other heavy elements, we simply assume that the proportions of all these elements relative to iron are the same as CI chondrites (Lodders 2003). This is a reasonable assumption, as demonstrated by the study of GD 362 and GD 40 (Zuckerman et al. 2007; Klein et al. 2010), and has the advantage of minimizing the consequences of unaccounted absorption from heavy elements other than iron. In other words, it is better to include absorption from additional metals rather than neglect their contribution completely. This was chosen over a time-consuming strategy involving navigation in a $N(Z)+2$ dimensional parameter space ($N(Z)$ elements, effective temperature, and surface gravity).

We use state-of-the-art model atmospheres based on a code similar to that described in Dufour et al. (2007) and Dufour (2007). We use calcium as a reference element and set the abundances of all elements with the proportions given by (Lodders 2003). This assumption needs to be verified a posteriori (see below). Our model grid covers a range from $T_{\text{eff}} = 13,000$ to 16,000 K in steps of 500 K, $\log g = 7.5$ to 9.0 in steps of 0.5 dex, and from $\log(\text{Ca}/\text{He}) = -5.5$ to -7.0 in steps of 0.5 dex. Additional models with traces of hydrogen have also been calculated. All models are calculated with the standard ML2 parametrization of the convective efficiency, but with a mixing length $\alpha = 1.25$ (Beauchamp et al. 1999).

We first start our fitting procedure by assuming the canonical value $\log g = 8.0$, but other values of the surface gravity ultimately had to be explored (see below). We evaluated, as explained above, the effective temperature and the iron abundance by fitting the optical spectra. If the lines of a given heavy element are found to be in disagreement with the observations, we readjust its abundance accordingly and a new model is recalculated with the new abundances in a self-consistent way. It is found that small variations of the abundances of elements other than iron have only a marginal impact on the thermodynamic structure of the star. Our inferred parameters are thus not sensitive to our initial assumptions.

However, we noticed that it was not possible to get a satisfactory simultaneous fit to the Mg I and Mg II lines under the assumption of $\log g = 8.0$. For example, a good fit to the various Mg II lines could be achieved only at the expense of a very bad fit to the Mg I doublet ($\lambda\lambda$ 3832, 3838), the latter being not strong enough for the assumed atmospheric parameters. This could have been an indication that the effective temperature was overestimated, but the much lower value needed to reconcile the Mg I and Mg II line strengths was clearly incompatible with the He I and Fe I/Fe II line profiles. Our first idea was that the thermodynamic structure of our model was wrong due to one of the assumptions about the composition, but models calculated by including only the observed elements were essentially identical to the ones with all the elements included. We also explored the parameter space to see if another combination of abundances and effective temperature could solve that problem, but no solutions were found.

Another way to favor the formation of Mg I relative to Mg II is to increase the atmospheric pressure. This can

be achieved if the surface gravity is allowed to increase in our fitting procedure. In a manner similar to that described above, we find that the Mg I and Mg II lines can be fitted simultaneously (as well as the He I, Fe I, and Fe II lines) if we increase the surface gravity to $\log g = 8.5$. Slightly larger/lower values of $\log g$ (compensated with an accordingly larger/lower effective temperature) can also accommodate simultaneously the Mg I and Mg II lines, but then the He I lines fit is not as good. Our derived mass determination thus relies heavily on the magnesium lines and the somewhat uncertain He I line profiles (usually attributed to the treatment of van der Waals broadening).

Trends of higher mass at low effective temperature for DB stars has raised concerns in the literature about the validity of the derived masses from He I lines. However, as clearly shown in Limoges & Bergeron (2010, see their Figure 7), it seems that the spread in mass is probably real after all. Since a higher than average surface gravity best fits both the He I lines and the Mg lines, we have a high confidence that J0738+1835 is indeed relatively massive. The debate will be settled when a trigonometric parallax measurement and better broadening theories become available, but until that happens, we consider our solution as the best compromise.

There appears to be large discrepancies in the predicted line strength of a few iron lines, the most noticeable being that of Fe II $\lambda 4173.46$ and near 5200 \AA (see Figure 3 and 4). These discrepancies cannot be eliminated even by varying significantly from our optimal solution the surface gravity and the effective temperature of our model. It is most probable that this is a manifestation of the uncertainties in the atomic data, $\log gf$ and Stark broadening parameters in particular, used in our calculation (we used the well known Kurucz linelists). We calculated a posteriori a synthetic spectrum using the Vienna Atomic Line Database (VALD) lists. Using these data helps to partly reduce the discrepancies for a few iron lines (for example, the depth of the Fe II $\lambda 4173.46$ is reduced by half) but does not alter the abundance determinations for any elements on average. Since our fit is based on numerous iron lines, these few discrepant lines have a relatively weak weight on the iron abundance determination and we present our final solution using the Kurucz linelist for consistency with the rest of our analysis.

We note that the assumption on the abundance of heavy elements described above also predicts weak lines of sodium (the Na D lines) that are blended with the He I $\lambda 5876$ line. There appear to be a feature in the red wing of the He I line that is consistent with the expected lines strength but given the signal-to-noise ratio of our observations and the weakness of the presumable lines, we shy away from claiming a detection. Two weak lines of Cr and Ti are also barely predicted at a level comparable to the signal-to-noise ratio of our observations. Future observations with higher signal-to-noise and higher resolution (as well as in other part of the electromagnetic spectrum) should eventually confirm their presence.

Our final solution is presented in in Table 1 while our best fit model spectra are shown in Figures 3 and 4. Uncertainties obtained from the covariance matrix are unrealistically small. These represent only internal errors

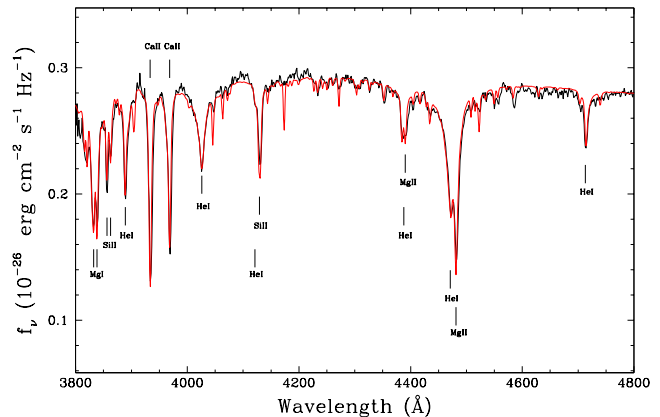


FIG. 3.— MMT spectrum (in black) and our best fit model (red line). The strongest lines are indicated by tick marks. All the other numerous non-identified lines are from iron. They have not been marked for clarity. In order to take into account uncertainties on the slope of the continuum due to extinction and flux calibration, a small linear and quadratic term were also included in the fitting procedure.

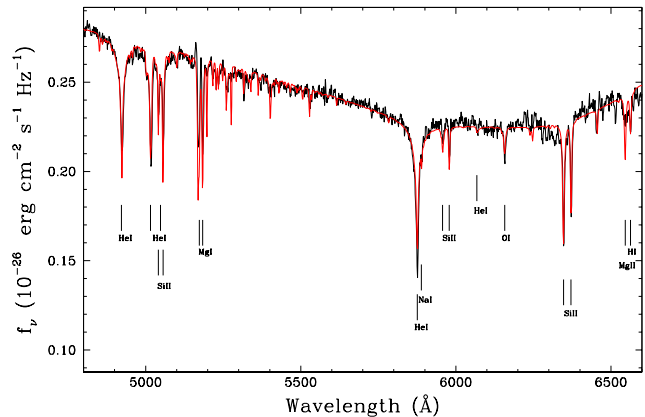


FIG. 4.— Same as Figure 3, but for the red part of the spectrum. Note that due to second order contamination longward of 5900 \AA , a second-order polynomial fit has been applied to the model spectrum continuum.

and thus underestimate the real uncertainties. We thus evaluate the uncertainties on the model parameters by calculating a series of models with various parameters near our optimal solution. The constraint from fitting simultaneously the Mg I, Mg II and He I lines dominates the errors on the effective temperature and surface gravity, which we evaluate to be about 300 K and 0.2 dex respectively. The uncertainties on the element abundances must also take into account these uncertainties. In a similar manner to that described in Klein et al. (2010), we varied the model T_{eff} and $\log g$ by their uncertainties, one at a time, to evaluate the corresponding errors on the various element abundances. The final uncertainties on the abundances presented in Table 1 are the sum of the errors added in quadrature. Those uncertainties are then properly propagated for the determination of the errors on the cooling age, luminosity, mass, radius and distance

TABLE 1
STELLAR PARAMETERS FOR SDSS
J0738+1835

Parameter	Value
T_{eff} (K)	13600 ± 300
$\log g$	8.5 ± 0.2
M_{WD}/M_{\odot}	0.907 ± 0.128
$M_{\text{init}}/M_{\odot}$	4.4 ± 1.0^a
R/R_{\odot}	0.00886 ± 0.0015
$\log L/L_{\odot}$	-2.62 ± 0.14
D	$136 \text{ pc} \pm 22$
Cooling Age	$595 \text{ Myr} \pm 219$
$\log \text{H}/\text{He}$	-5.7 ± 0.3
$\log \text{O}/\text{He}$	-4.0 ± 0.2
$\log \text{Mg}/\text{He}$	-4.7 ± 0.2
$\log \text{Si}/\text{He}$	-4.9 ± 0.2
$\log \text{Ca}/\text{He}$	-6.8 ± 0.3
$\log \text{Fe}/\text{He}$	-5.1 ± 0.3
$\log(M_{\text{He}}/M_{\star})$	$-6.5 +0.8/-0.25$

^a Initial mass of the main sequence progenitor calculated using the Initial-Final Mass Relation of Williams et al. (2009)

of the star (obtained by determining the solid angle from the *ugriz* photometry). The evolutionary models used are similar to those described in (Fontaine et al. 2001) but with C/O cores, and thickness of the helium and hydrogen layers of respectively $q(\text{He}) = 10^{-2}$ and $q(\text{H}) = 10^{-10}$, which are representative of helium-rich atmosphere white dwarfs.

Finally, we calculated a posteriori a model with the final abundances of only the observed elements. We find that the resulting synthetic spectrum is practically identical to the one with all elements included. This is not surprising given that Fe, Mg, Si, O, and Ca account for more than 95% of the contaminants by mass for Bulk Earth (a similar proportion was also found for GD 40, Klein et al. 2010). A similar proportion will probably be retrieved for J0738+1835 when high resolution observations become available (ultraviolet observations should also be helpful).

3.2. Convection Zone Models

In order to evaluate the total amount of heavy material mixed in the outer layers of J0738+1835, we need to know the mass of the helium convection zone into which the metals are diluted. Estimates of this mass can readily be obtained using the Montréal white dwarf building codes that were developed over the years (see, e.g., Brassard & Fontaine 1994; Fontaine et al. 2001), and which have been maintained at the state-of-the-art level. One possible option offered by these codes is to compute complete, but static, stellar structures with a luminosity profile closely following the mass profile, as appropriate for cool white dwarfs shining through the loss of thermal energy. This is what we adopted here.

To ease the comparison with the spectroscopic observations, we further selected the option of fixing the surface gravity and the effective temperature (as well as the compositional stratification and the core composition) in these stellar model calculations. We also assumed relatively thick helium envelopes in these models, $\log(1 - M_{\text{He}}/M_{\star}) = -3.0$, much thicker than the superficial outer convection zone due to helium partial ionization.

TABLE 2
FRACTIONAL MASS OF THE CONVECTION ZONE ($\log M_{\text{He}}/M_{\star}$), FOR VARIOUS SURFACE GRAVITIES, EFFECTIVE TEMPERATURES, AND CONVECTIVE EFFICIENCIES

$\log g$	T_{eff} (K)	ML2/ $\alpha = 0.6$	ML2	ML3
7.5	13000	-4.344	-4.301	-4.259
	14000	-4.604	-4.518	-4.454
8.0	13000	-5.367	-5.324	-5.324
	14000	-5.543	-5.500	-5.457
8.5	13000	-6.447	-6.447	-6.425
	14000	-6.580	-6.558	-6.537
9.0	13000	-7.661	-7.661	-7.661
	14000	-7.729	-7.707	-7.707

Since the presence of heavy elements does affect somewhat the extent of the convection zone, models with an envelope composition consisting of helium and homogeneous traces of metals were considered along with more standard models having pure helium envelopes. We retained the results for a metallicity of $Z = 0.001$ in what follows.

We investigated also how M_{He}/M_{\star} depends on the assumed convective efficiency. This is because, as was first shown by Bergeron et al. (1995), the calibration of the mixing-length derived in the atmospheric layers (by comparing optical and UV observations) does not apply at the base of the convection zone, where the flux of settling heavy elements determines the observable abundances. In that case, the calibration is best obtained by comparing the effective temperatures at the blue edge of an instability strip as inferred from nonadiabatic pulsation calculations with the values derived from spectroscopy. In the case of pulsating H-rich (DA) white dwarfs, Bergeron et al. (1995) found that the convective efficiency increases with depth, from the atmospheric layers to the bottom of the convection zone, so that a variable mixing length is required to account for both the spectroscopic and pulsational measurements. Unfortunately, the calibration based on pulsational properties is still uncertain, particularly for the He-atmosphere white dwarfs (see, e.g., Fontaine & Brassard 2008), so we decided to consider three different plausible versions of the mixing-length theory for constraining the mass of the outer convection zone in J0738+1835.

The results of our calculations are presented in Table 2 for values of $\log g$ and T_{eff} in the vicinity of those found spectroscopically for J0738+1835. Our calculations indicate that the mass of the helium convection zone in that regime is, fortunately, only weakly dependent on the effective temperature and on the convective theory flavor used in the stellar models. However, a strong dependency on the surface gravity is found, M_{He}/M_{\star} decreasing significantly as the surface gravity increases. Using our atmospheric parameters, we estimate that the mass of the helium convection zone lies somewhere between $10^{-5.70}M_{\star}$ and $10^{-6.75}M_{\star}$. Correspondingly, the lower limits on the mass of the polluting body (i.e. the sum of the masses of the detected elements in Table 1) are between 2.7×10^{23} g and 2.4×10^{24} g, with a value of 4.3×10^{23} g corresponding to $\log g = 8.5$.

This is close to the mass of Ceres (9.4×10^{23} g) and is about an order of magnitude more than the

amount of metals found in the convection zones of GD 40 (Klein et al. 2010) and GD 362 (Koester 2009) (3.6×10^{22} g and 1.8×10^{22} g, respectively), and comparable to the amount found in HS 2253+8023 (Jura 2006) which is, however, based solely on the derived Fe abundance from an *IUE* spectrum (Friedrich et al. 1999). Because an unknown period of time has elapsed since the accretion process has started, we do not know what fraction of the material has already sunk out of sight below the base of the convection zone and, therefore, this estimate for the total mass of heavy elements represents a lower limit on the mass of the body responsible for this large pollution. Given this, and the fact that another yet unknown quantity of material is still orbiting the star in the form of a debris disk (see below), it is safe to presume that the object that was tidally destroyed by J0738+1835 was at least as large as the dwarf planet Ceres.

This lower limit is sensitive to the determined value of the surface gravity. It will thus be of utmost importance to determine the surface gravity with greater accuracy than is currently possible in order to precisely constrain the mass of the asteroid/dwarf planet that causes the pollution in J0738+1835. A good trigonometric parallax measurement should help to reduce this uncertainty significantly.

3.3. Infrared Photometry and Disk Model

The next step was to determine if an accretion disk is still present around J0738+1835, which would be revealed by an infrared excess. We thus obtained infrared *JHK* photometry with the 8 m Gemini North telescope in Hawaii. Our observations, presented in Figure 5, clearly reveal a near-IR excess.

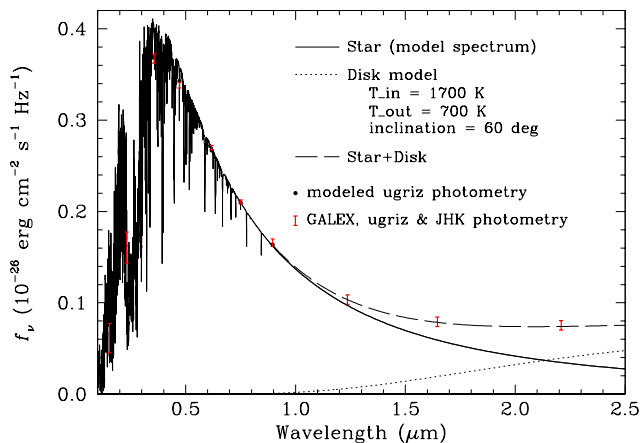


FIG. 5.— Photometric measurements in the GALEX, *ugriz* and *JHK* bands compared to models of the star and the debris disk.

Given the fact that most heavily polluted white dwarfs have debris disks, our target is likely to have a disk as well. If the near-infrared excess is due to a companion star, this star would have $M_K = 12.35$ mag; an L6 dwarf (Leggett et al. 2002). Such a companion would have $H - K = 0.6-0.9$ mag. The near-infrared excess around our target (after subtracting the contribution from the stellar photosphere) has a $H - K$ color of 1.33 mag, incompatible

with an L6 dwarf or any other M, L, and T dwarfs studied by Leggett et al. (2002). Therefore, the infrared excess around our target is best explained by the presence of a dusty debris disk rather than a brown dwarf companion.

We fit the infrared excess around J0738+1835 using the optically thick flat-disk models of Jura (2003). Using the effective temperature, radius, and distance estimates for the white dwarf (see Table 1), we created a grid of disk models with inner temperatures 1000-1800 K, outer temperatures 300-900 K (in steps of 100 K), and inclination angles $15^\circ-75^\circ$ (in steps of 15°). The model that best fits the infrared photometry has $T_{in} = 1700$ K, $T_{out} = 700$ K, and an inclination angle of 60° . However, since we only have near-IR data, the outer temperature is not well constrained, and these parameters change depending on the assumed inclination. For example, if the inclination angle is assumed to be 75° , then the best fit model has $T_{in}=1600$ K and $T_{out}=300$ K. Nevertheless, the near-IR data can be explained with a reasonable set of parameters for a dusty disk, indicating that the accretion process is most probably occurring at present. An inner temperature of 1700 K is somewhat unusual for disks around white dwarfs. However, the near-infrared flux excess around J0738+1835 is similar to the excess seen around the white dwarf GD 56 (Kilic et al. 2006). A flat-disk model with an inner temperature of 1700 K is required to explain the observed excess around GD 56 (Jura et al. 2007a). A better fit to the near-infrared data for GD 56 can be obtained if the disk is substantially warped or puffed up by the gravitational field of a planet (Jura et al. 2009). Similar processes may be responsible for the observed near-infrared flux distribution of the disk around J0738+1835. Mid-infrared observations will be useful to check the flat-disk models for this target.

Unfortunately, the total mass of the disk cannot be determined for an opaque ring. Masses for the dust disks around G29-38 and GD 362 have been estimated from models of the mid-infrared emission (Reach et al. 2005; Becklin et al. 2005). Based on the choice of optically thin or thick models, these disks hold $\sim 10^{19} - 10^{24}$ g of material. The disk around J0738+1835 is likely to hold a similar amount of material as well. Hence, the combined mass of the metals in the surface convection zone and the dust disk is on the order of $4-14 \times 10^{23}$ g, equivalent to the mass of a dwarf planet.

4. DISCUSSION AND CONCLUSION

According to the accretion/diffusion scenario (Dupuis et al. 1992, 1993a,b), a steady state abundance for a given heavy element is rapidly reached after the accretion process starts. Under those circumstances, the ratio of abundances measured spectroscopically in the photosphere of J0738+1835 can be related, unlike the case of HS 2253+802 which shows no disk (Farihi et al. 2009), to that of the incoming disk material.

It is interesting to note that the mass ratios of the most abundant heavy elements found in J0738+1835, namely O, Mg, Si and Fe, are very similar to that found in GD 40, which has an atmosphere polluted with debris coming from a body with an Earth-like composition (Klein et al. 2010). However, calcium is depleted in J0738+1835 by a factor of 4, perhaps indicating that mantle/crust differentiation has occurred before the crust was lost. More-

over, if we assume that the total amount of hydrogen present in the atmosphere of J0738+1835 originates from the last polluting event only, we can place an upper limit of $\sim 1\%$ by mass on the water or ice content of the polluting body. This is a surprisingly low amount considering that most asteroids in our solar system contain large quantities of ice on their surface. This might indicate that the parent body was sufficiently close to the progenitor red giant star for thermal processes to have evaporated most of the ice or water initially present (Jura & Xu 2010). Thus it is possible that the surface of the orbiting body was significantly altered in the late stages of stellar evolution, but at this point it is premature to quantify this effect. Given the uncertainties on the atmospheric parameters, we shall refrain from speculating further on the true fate of the body that polluted the atmosphere of J0738+1835. However, when parallax and higher resolution spectroscopy observations become available, J0738+1835 will become a perfect testbed for a precise study of not only the abundances of the polluting extrasolar body, but also of the effects of processes such as crust differentiation and thermal heating.

It is worth noting that medium resolution observations of GD 362 and GD 40 revealed only relatively weak absorptions of Ca, Mg, and Fe in the optical (Figure 1). It was only when Keck high resolution spectra became available that a myriad of elements were uncovered, providing extremely valuable information about the accreted material. Given that J0738+1835's medium resolution spectrum is showing even stronger metallic absorption

lines than in the cases of GD 362 and GD 40, further high resolution observations in the optical and ultraviolet to study elemental abundances as well as at longer wavelengths to characterize the debris disk are highly desirable. These observations will undoubtedly offer an opportunity to study the composition of an extrasolar dwarf planet with unprecedented accuracy.

This work was supported in part by NSERC Canada and FQRNT Québec. P.D is a CRAQ postdoctoral fellow, and P.B is a Cottrell Scholar of Research for Science Advancement. G.F. acknowledges the contribution of the Canada Research Chair Program. MK acknowledges support from NASA through the Spitzer Space Telescope Fellowship Program, under an award from Caltech. Based on observations obtained at the MMT and Gemini Observatory. The MMT is a joint facility of the Smithsonian Institution and the University of Arizona. The Gemini observatory is operated by the Association of Universities for Research in Astronomy, Inc., under a cooperative agreement with the NSF on behalf of the Gemini partnership: the National Science Foundation (United States), the Science and Technology Facilities Council (United Kingdom), the National Research Council (Canada), CONICYT (Chile), the Australian Research Council (Australia), Ministerio da Ciencia, Tecnologia (Brazil) and Ministerio de Ciencia, Tecnologia e Innovacion Productiva (Argentina).

REFERENCES

- Aannestad, P. A., Kenyon, S. J., Hammond, G. L., & Sion, E. M. 1993, *AJ*, 105, 1033
- Beauchamp, A., Wesemael, F., Bergeron, P., Fontaine, G., Saffer, R. A., Liebert, J., & Brassard, P. 1999, *ApJ*, 516, 887
- Becklin, E. E., Farihi, J., Jura, M., Song, I., Weinberger, A. J., & Zuckerman, B. 2005, *ApJ*, 632, L119
- Bergeron, P., Wesemael, F., Lamontagne, R., Fontaine, G., Saffer, R. A., & Allard, N. F. 1995, *ApJ*, 449, 258
- Brassard, P., & Fontaine, G. 1994, *IAU Colloq. 147: The Equation of State in Astrophysics*, 560
- Debes, J. H., & Sigurdsson, S. 2002, *ApJ*, 572, 556
- Dufour, P., et al. 2007, *ApJ*, 663, 1291
- Dufour, P. 2007, Ph.D. Thesis, Université de Montréal
- Dupuis, J., Fontaine, G., Pelletier, C., & Wesemael, F. 1992, *ApJS*, 82, 505
- Dupuis, J., Fontaine, G., Pelletier, C., & Wesemael, F. 1993a, *ApJS*, 84, 73
- Dupuis, J., Fontaine, G., & Wesemael, F. 1993b, *ApJS*, 87, 345
- Eisenstein, D. J., et al. 2006, *ApJS*, 167, 40
- Farihi, J., Barstow, M. A., Redfield, S., Dufour, P., & Hambly, N. C. 2010, arXiv:1001.5025
- Farihi, J., Jura, M., & Zuckerman, B. 2009, *ApJ*, 694, 805
- Fontaine, G., & Brassard, P. 2008, *PASP*, 120, 1043
- Fontaine, G., Brassard, P., & Bergeron, P. 2001, *PASP*, 113, 409
- Friedrich, S., Koester, D., Heber, U., Jeffery, C. S., & Reimers, D. 1999, *A&A*, 350, 865
- Gianninas, A., Dufour, P., & Bergeron, P. 2004, *ApJ*, 617, L57
- Jura, M. 2003, *ApJ*, 584, L91
- Jura, M. 2006, *ApJ*, 653, 613
- Jura, M., Farihi, J., & Zuckerman, B. 2007, *ApJ*, 663, 1285
- Jura, M., Farihi, J., Zuckerman, B., & Becklin, E. E. 2007, *AJ*, 133, 1927
- Jura, M. 2008, *AJ*, 135, 1785
- Jura, M., Farihi, J., & Zuckerman, B. 2009, *AJ*, 137, 3191
- Jura, M., & Xu, S. 2010, arXiv:1001.2595
- Kilic, M., & Redfield, S. 2007, *ApJ*, 660, 641
- Kilic, M., von Hippel, T., Leggett, S. K., & Winget, D. E. 2005, *ApJ*, 632, L115
- Kilic, M., von Hippel, T., Leggett, S. K., & Winget, D. E. 2006, *ApJ*, 646, 474
- Klein, B., Jura, M., Koester, D., Zuckerman, B., & Melis, C. 2010, *ApJ*, 709, 950
- Koester, D., & Wilken, D. 2006, *A&A*, 453, 1051
- Koester, D., & Wolff, B. 2000, *A&A*, 357, 587
- Koester, D. 2009, *A&A*, 498, 517
- Leggett, S. K., et al. 2002, *ApJ*, 564, 452
- Leggett, S. K., et al. 2006, *MNRAS*, 373, 781
- Limoges, M.-M., & Bergeron, P. 2010, *ApJ*, 714, 1037
- Lodders, K. 2003, *ApJ*, 591, 1220
- Massey, P., Strobel, K., Barnes, J. V., & Anderson, E. 1988, *ApJ*, 328, 315
- Paquette, C., Pelletier, C., Fontaine, G., & Michaud, G. 1986, *ApJS*, 61, 197
- Reach, W. T., Kuchner, M. J., von Hippel, T., Burrows, A., Mullally, F., Kilic, M., & Winget, D. E. 2005, *ApJ*, 635, L161
- von Hippel, T., Kuchner, M. J., Kilic, M., Mullally, F., & Reach, W. T. 2007, *ApJ*, 662, 544
- Voss, B., Koester, D., Napiwotzki, R., Christlieb, N., & Reimers, D. 2007, *A&A*, 470, 1079
- Williams, K. A., Bolte, M., & Koester, D. 2009, *ApJ*, 693, 355
- Wolff, B., Koester, D., & Liebert, J. 2002, *A&A*, 385, 995
- Zuckerman, B., Koester, D., Melis, C., Hansen, B. M., & Jura, M. 2007, *ApJ*, 671, 872